Colloid Polym Sci (2005) 283: 1116–1122
DOI 10.1007/s00396-004-1257-2

Szilvia Papp
Imre Dékány

Colloid chemical characterisation of layered titanates, their hydrophobic derivatives and self-assembled films

Received: 30 August 2004
Accepted: 24 November 2004
Published online: 15 January 2005

S. Papp · I. Dékány
Nanostructured Materials Research Group of the Hungarian Academy of Sciences, University of Szeged, 6720 Aradi v. t. 1, Szeged, Hungary

I. Dékány (✉)
Department of Colloid Chemistry, University of Szeged,
6720 Aradi v. t. 1, Szeged, Hungary
E-mail: i.dekany@chem.u-szeged.hu
Tel.: +36-62-544210
Fax: +36-62-544042

Abstract $Na_2Ti_3O_7$, with layered structure, was prepared from a 1:3 molar mixture of powdered Na_2CO_3 and TiO_2 by heating at 800 °C for 2 h. The Na^+ ions were exchanged for H^+ ions by hydrochloric acid treatment; next, *n*-butylamine, *n*-octylamine, *n*-decylamine or *n*-dodecylamine were incorporated at pH = 3.6–3.8. It was proven by XRD measurements that, as the length of the alkyl chain of the amines was increased, smaller amounts of amines were intercalated under identical conditions. $H_2Ti_3O_7$ samples dispersed in liquids of various compositions and polarities were used for the preparation of self-assembled titanate/polymer films for further sensor applications. Titanates, their composites with alkyl amines and the self-assembled hybrid structures were characterized by X-ray diffraction, thermoanalytical, optical, electron and atomic force microscopic measurements.

Keywords Trititanate · Self-assembling · Hybrid films · Titanate/polymer nanocomposites

Introduction

The preparation of layered titanates and the evaluation of their structural properties are significant tasks of material science. The physical and chemical properties of layered titanates are different from those of the widely studied titania nanoparticles. Detailed structural characterizations of titanates of various compositions have appeared in the literature since as early as the 1960s. Andersson and Wadsley published the crystallographic parameters of K-dititanate and Na-dititanate in 1961 [1, 2]. Easteal and Udy prepared K_2TiO_3 (K-metatitanate), $K_2Ti_2O_5$ (K-dititanate), $K_2Ti_4O_9$ (K-tetratitanate) and $K_2Ti_6O_{13}$ (K-hexatitanate) and characterized them by IR and far-IR spectroscopy [3]. Titanates have layered structure and function as ion exchangers. The ion exchange properties of titanates and their ion-exchanged forms have been and are being studied by numerous authors [4–13]. Knowledge of these characteristics is very important, because these make possible the introduction of guest molecules into the interlamellar space and generating intercalation compounds. Izawa et al. [4] experienced that Na- and K-titanates do not directly react with organic cations. After partial exchange of alkali ions for H^+ (yielding $NaHTi_4O_9$ and $KHTi_3O_7$), they prepared *n*-alkylammonium complexes of tri- and tetratitanates by replacement of H^+ ions by alkylamines. They observed that the rate of incorporation decreased with increasing amine chain length. Other researchers partially achieved the replacement of alkali ions directly by alkylammonium ions [6, 7]. Ogawa and Takizawa used macrocyclic compounds ([2.2.2]-crypt- and, 18-crown-6) to facilitate the incorporation, via ion exchange, of alkylammonium chlorides into the semiconductive $K_2Ti_4O_9$ [13]. Macrocyclic compounds can undergo complexation with exchangeable cations, facil-

itating the incorporation of amines. Similar to the already well-known clay/polymer composites, titanate may also intercalate macromolecules. Sukpirom and Lerner prepared nanocomposites with PEO and PVP polymers by adding aqueous polymer solutions to titanate previously exfoliated by alkylamine [14, 15]. The effect of the particle size of TiO_2 on the ion exchange capacity and morphology of the titanates formed was recently studied [16], and the ion exchange capacity was found to increase with decreasing size.

Based on the favourable photocatalytic properties of TiO_2, attempts have been initiated to study titanates in similar reactions [17–27]. Cheng et al. [17] performed decomposition of phenol on *K*-tetratitanate with half the efficiency of TiO_2. The photocatalytic activity of titanates has been improved by the incorporation of semiconductive nanoparticles. The composites obtained were suitable for the decomposition of organic molecules as well as for splitting water [18–26]. Sato and coworkers [20–24] incorporated semiconductive oxides, sulphides and Pt nanoparticles into the interlamellar space. They first incorporated propylamine and later, Cd^{2+} and Zn^{2+} ions into $H_2Ti_4O_9$ and reacted the incorporated compounds with H_2S. They also incorporated Fe_2O_3 into titanate by UV irradiation of the ion-exchanged support. They prepared a Pt-TiO_2/titanate composite by incorporating $[Pt(NH_3)_4]$ into titanate followed by UV irradiation, replacement of TiO_2 by propylamine and the addition of the TiO_2 sol to the support. They succeeded in liberating significant amounts of hydrogen by splitting water with the help of their composites. Hydrogen liberated from these catalyst suspensions prepared in water or in 0.1 M Na_2SO_4 or Na_2SO_3 by irradiation with visible light was quantified in a gas burette. The most extensive generation of hydrogen was recorded in suspensions of the $H_2Ti_4O_9$/$Cd_{0.8}Zn_{0.2}S$ composite in a medium containing Na_2S. Machida et al. [25] also generated hydrogen from aqueous methanol using tri- and tetratitanate pillared with SiO_2 and Al_2O_3 and titanates in which Ti^{4+} was partially replaced by heavy metals ions. Self-assembled films were also prepared from titanates, for the purpose of more practical applicability and higher efficiency [27, 28]. Titanium nanoplates are applied to the surface of substrates, usually glass plates, with the help of a polymer binding to the glass surface (PEI), and alternating layers of polymer and titanate were superposed by the immersion technique.

The application of titanates as oxygen electrodes of gas sensors has also been examined [29–31]. Holzinger prepared two types of reference electrodes: one was made by mixing $Na_2Ti_6O_{13}$, TiO_2 in different ratios and gold powder and subsequent sintering at 1,050 °C, the other was prepared in the same way, but using $Na_2Ti_3O_{17}$ instead of TiO_2. One surface of the reference electrode pellet was contacted with gold foil [31].

In this study, we present the preparation of hydrogen titanate and its intercalation with alkylamines. Since this is a material with layered structure, it has a superb capability for self-arrangement and is suitable for the preparation of ultrathin layers. We demonstrate the self-arranging ability of titanates, which may also render them suitable for utilization as efficient photocatalysts and sensors. We also show the analogy between the intercalation and self-arranging properties of layer silicates and titanates.

Materials

Sodium titanate ($Na_2Ti_3O_7$) was prepared by heating sodium carbonate decahydrate ($NaCO_3 \cdot 10H_2O$, Reanal) and titanium dioxide (TiO_2, d $\sim$ 25 nm, a two-phase mixture containing 75% anatase and 25% rutile, Degussa P25) in a 99.9% platinum crucible. Hydrogen titanate was obtained from sodium titanate by the addition of hydrogen chloride solution (HCl, 37 wt%, Reanal). Compounds incorporated among the titanate layers were n-alkylamines ($n = 4$, 8, 10, 12, Loba Chemie).

Preparation of layered sodium trititanate

Layered $Na_2Ti_3O_7$ was prepared from a 1:3 molar mixture of Na_2CO_3 and TiO_2 by heating at 800 °C in a tube furnace with programmed heating (Fig. 1). The heat-up rate of the furnace was 10 °C/min and heating was performed in nitrogen flow. The sodium trititanate obtained was stirred continuously in 500 ml of 1 M hydrochloric acid at room temperature. *H*-titanate formed was centrifuged and exchanged Na^+ ions were removed by washing three times in distilled water and centrifugation. The sample was dried at 60 °C and ground. Specific surface area determined by N_2 adsorption measurement at 77 K was 2.1 m^2/g for $Na_2Ti_3O_7$ and 6.1 m^2/g for $H_2Ti_3O_7$, calculated by the BET method.

Preparation of *N*-alkylammonium titanates

The cation exchange capability of hydrogen titanate was measured for incorporating *n*-butylammonium ions in the interlamellar space. Structural changes of the titanate were followed by X-ray diffraction measurements. 2 g of $H_2Ti_3O_7$ was suspended in 100 ml of 4.5–34 g/l amine, at pH = 3.6–3.8, left to stand at 65 °C for 6 days, filtered and dried at room temperature. The octylamine solution was prepared in an ethanol-water mixture, whereas decylamine and dodecylamine solutions were made up in ethanol.

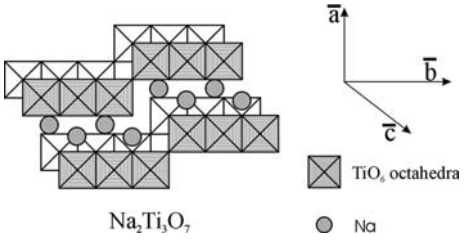

Fig. 1 Structure of layered sodium trititanate

Methods

1. XRD: X-ray diffraction measurements were taken on a Philips PW 1820 diffractometer (CuK_α radiation, 40 kV, 30 mA) in the 2Θ range $1° \leq 2\Theta \leq 30°$. The basal spacings d_L were calculated from the first (001) Bragg reflections by using the PW 1877 automated powder diffraction software.
2. Transmission electron microscopy (TEM): Images were made using a Philips CM-10 transmission electron microscope with an accelerating voltage of 100 kV. Aliquots of the ethanol suspensions of the samples were dropped on copper grids (diameter 2 mm) covered with Formwar foil, which were then left to stand for 3–40 s and then transferred into the microscope. Particle size distribution was determined by using the UTHSCS1A Image Tool program.
3. Atomic Force Microscope (AFM): The AFM images were performed with the Nanoscope III (Digital Instruments, USA) piezo scanner with scanning capability of 12.5 μm in x and y direction and 3 μm in z direction, tapping type tip made of silicon (Veeco Nanoprobe Tips RTESP modell, 125 μm length, 300 kHz).
4. Thermal analysis: The measurements in the MOM Q-1500 D instrument were made in air, at 25–1,000 °C, with a heating rate of 5 °C/min.
5. Dynamic light scattering (DLS): SEM-633 goniometer (SEMATech) with a HeNe laser (wavelength 632.8 nm, angle of observation 90°), R.T.G. 12 channel logarithmic, digital photon correlator unit (SEMATech). The applied pinhole had a diameter of 50 μm, and the g_2 value was typically ~1.6.
6. UV-VIS spectroscopy: Uvicon 930 UV-VIS absorption spectrophotometer.
7. Nitrogen gas adsorption measurements: Gemini 2735 (Micromeritics) automated sorptometer at 77.4 ± 0.5 K in liquid nitrogen. Prior to measurements the samples were pretreated in vacuum at 393 K for 2 h. The sample vessel was loaded with ca. 0.1 g of samples.
8. Layer-by-layer (LBL) technique: Self-assembled films were prepared on glass surfaces, starting from

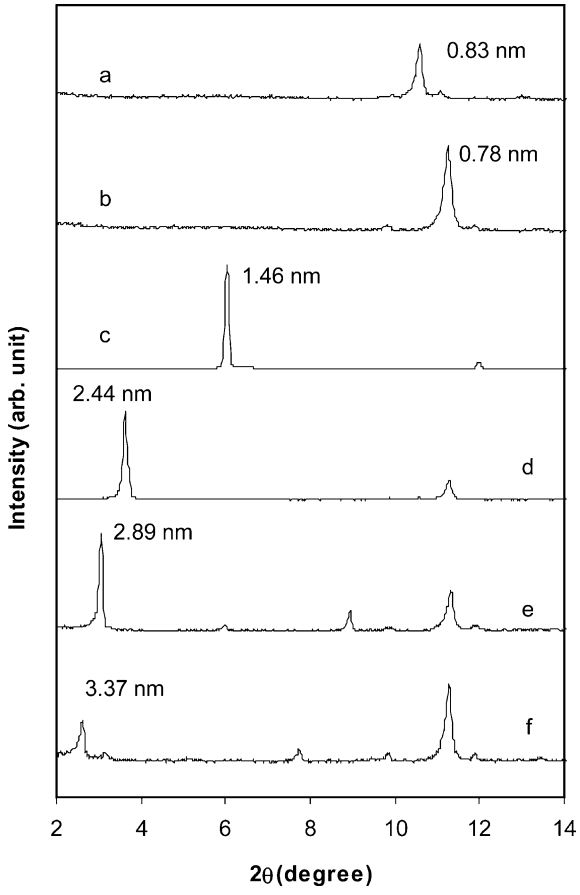

Fig. 2 XRD patterns of sodium and hydrogen trititanate, and intercalated titanates: **a** $Na_2Ti_3O_7$, **b** $H_2Ti_3O_7$, **c** butylamine/$H_2Ti_3O_7$, **d** octylamine/$H_2Ti_3O_7$, **e** decylamine/$H_2Ti_3O_7$, **f** dodecylamine/$H_2Ti_3O_7$

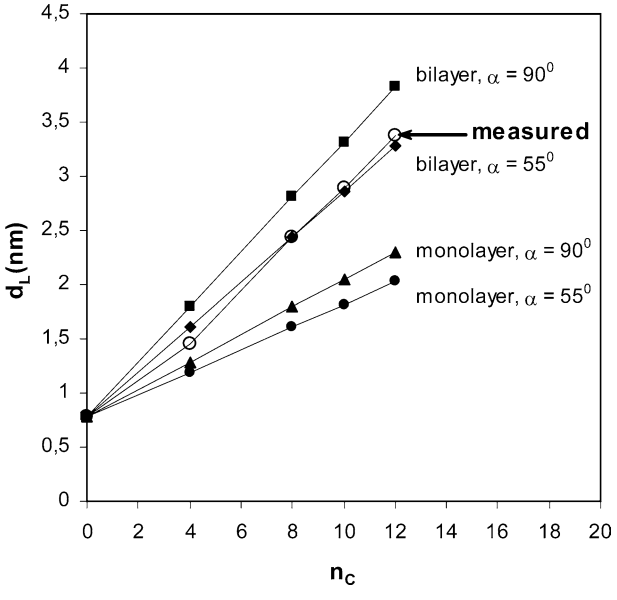

Fig. 3 Measured and calculated basal spacings of n-alkylamine titanates, n_c = number of carbon atoms of the alkyl chain

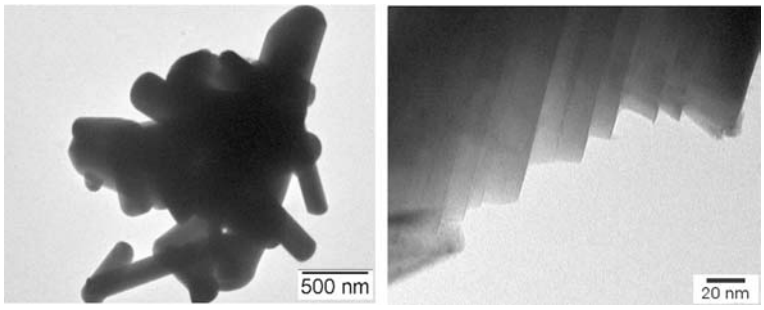

Fig. 4 TEM pictures of $Na_2Ti_3O_7$ (**a**) and $H_2Ti_3O_7$ (**b**)

aqueous (film 1) and *n*-propanol (film 2) dispersions of H-titanate. The surface of the glass was first cleaned in a 3:1 mixture of H_2SO_4 and H_2O_2 for 1 day. Films were prepared by dipping a glass substrate in colloidal suspension of the titanate nanosheets and poly(diallyldimethylammonium chloride) solution. To promote the adsorption of titanate sheets on the glass substrate surface was precoated with polyethylenimine (PEI) from 1 g/l aqueous solution. The repeated steps of one complete cycle were as follows: (1) Immersion of the precoated glass substrate into the suspension of negatively charged hydrogen trititanate nanosheets (0.5 wt%, pH = 9.5) for 15 min; (2) washing with water; (3) immersion in a diluted aqueous solution of poly(diallyldimethylammonium chloride) (PDDACl at 1 g/l suspension concentration, pH = 6.6) for 15 min and washing with water. The rate of immersion and withdrawal was 10 cm/min (see Fig. 8).

9. Determination of surface charge density: The suspensions of $H_2Ti_3O_7$ (0.1 g/l) were titrated with 0.05 mM hexadecylpyridinium chloride (HDPCl) solution and changes in their surface charge state were measured with a Mütec PCD device after shaking for 4 and 6 days.

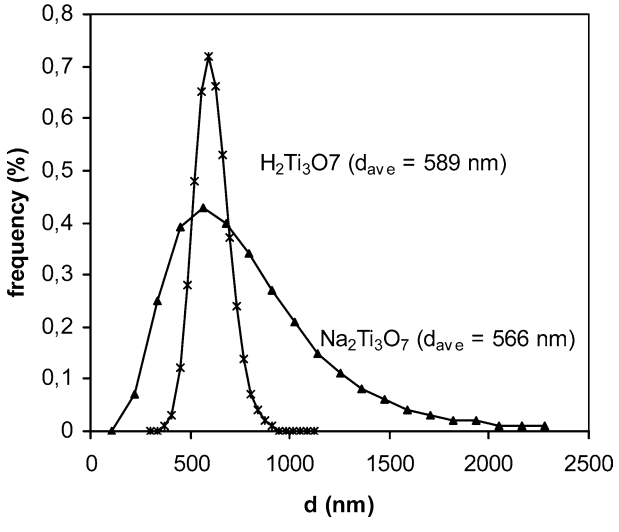

Fig. 5 Particle size distribution curves of $Na_2Ti_3O_7$and $H_2Ti_3O_7$ titanates calculated from DLS measurements

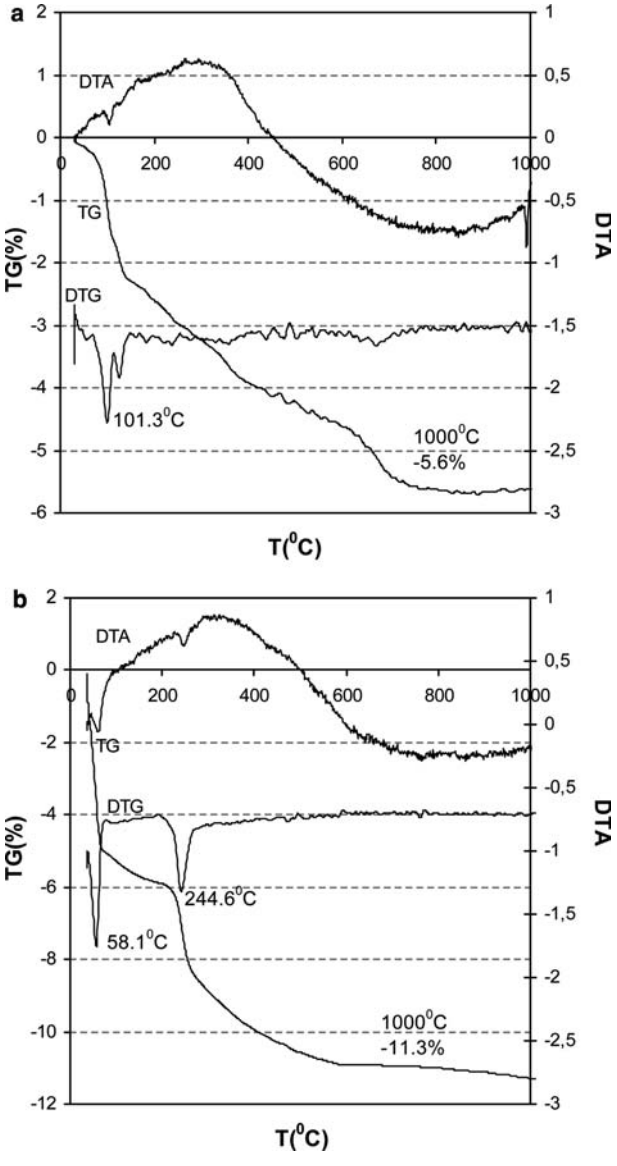

Fig. 6 Differential thermal analysis of $Na_2Ti_3O_7$ (**a**) and $H_2Ti_3O_7$ (**b**)

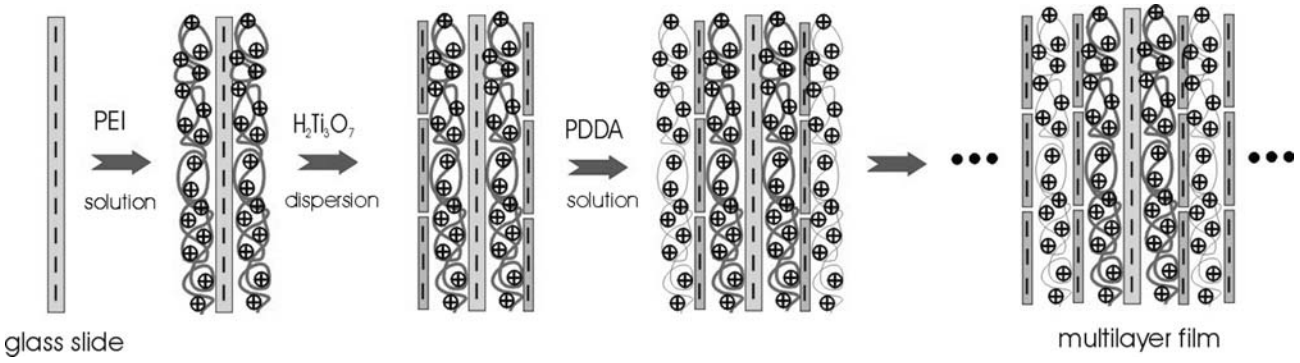

Fig. 7 Preparation of self-assembly films: purified glass slide dipping in PEI polymer solution; after rinsing in Millipore water dipping in titanate suspension; after rinsing in Millipore water dipping in PDDACl solution etc

Results and Discussion

After a 20-h heating of the Na_2CO_3/TiO_2 powder mixture at 800 °C, the basal spacing of $Na_2Ti_3O_7$ (100) appeared as a sharp peak at $d_L = 0.83$ nm, as given in reference [10] (Fig. 2a). Hydrochloric acid treatment shifts this reflection to $d_L = 0.78$ nm (Fig. 2b). When amines with alkyl chains of different lengths ($n_c = 4$, 8, 10, 12) are incorporated between the titanate layers, the basal spacing increases systematically (Fig. 2c-f). As the chain length is increased, lesser number of the amines can be incorporated between the layers, after 6 days . The $d_L = 0.78$ nm reflection of the unreacted titanate is seen after reaction with longer amines (Fig. 2c-f). With butylamine the basal spacing of 0.78 nm is not detectable any more (Fig. 2c), and the reaction is complete. The basal spacings for different arrangements of the alkyl chains were calculated after publications by Lagaly and coworkers [31–33]. Figure 3 shows calculated basal spacings based on monolayer and bilayer models and chain tilting angles $\alpha = 55°$ and 90° for $n_c = 4$, 8, 10, 12. Similarly to the situation in organophilized clay minerals, the alkyl chains of alkylamines most probably make a tilting angle of 55° with the lamellae. When the basal spacing is calculated assuming the presence of two layers of octylamine between two lamellae with $\alpha = 55°$ tilting angle: $d_L = 0.78$ nm + $(2 \times n_c \times 0.127$ nm $\times \sin 55°) =$ 2.44 nm at $n_c = 8$ (n_c is the number of carbon atoms in the alkyl chain) is obtained, which is identical with the basal spacing measured. It is clearly shown by Fig. 3 that this model fits well the experimental data in the examined chain length range.

Transmission electron micrographs (TEM) display the lamellar structure and the long rectangular shadow of both materials. The TEM picture of Na-titanate mostly displays aggregated groups of lamellae (Fig. 4a), whereas that of *H*-titanate shows isolated platelets (Fig. 4b). During the acid treatment bundles of Na-titanate lamellae are split to smaller units. The size of $Na_2Ti_3O_7$ and $H_2Ti_3O_7$ platelets is almost the same, their lateral dimensions are 150–500 nm and 500–2,500 nm, respectively.

Light scattering was measured in dilute aqueous suspensions (0.01 g/100 ml). The fast sedimenting Na-titanate was studied 10 min after being suspended, i.e. after sedimentation of the larger particles, we only

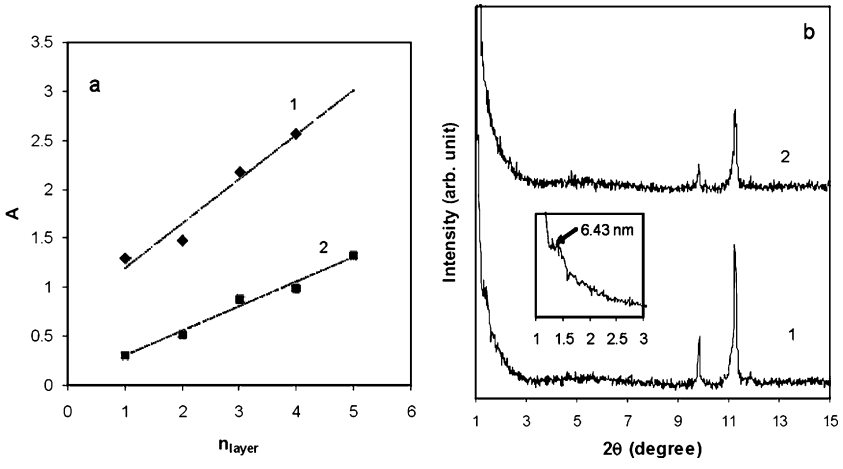

Fig. 8 **a** Absorbance values of self-assembled films built from aqueous (*1*) and from n-propanol (*2*) measured at $\lambda = 600$ nm. **b** XRD patterns of self-assembled films built from aqueous (*1*) and from *n*-propanol (*2*) after deposition of five layers

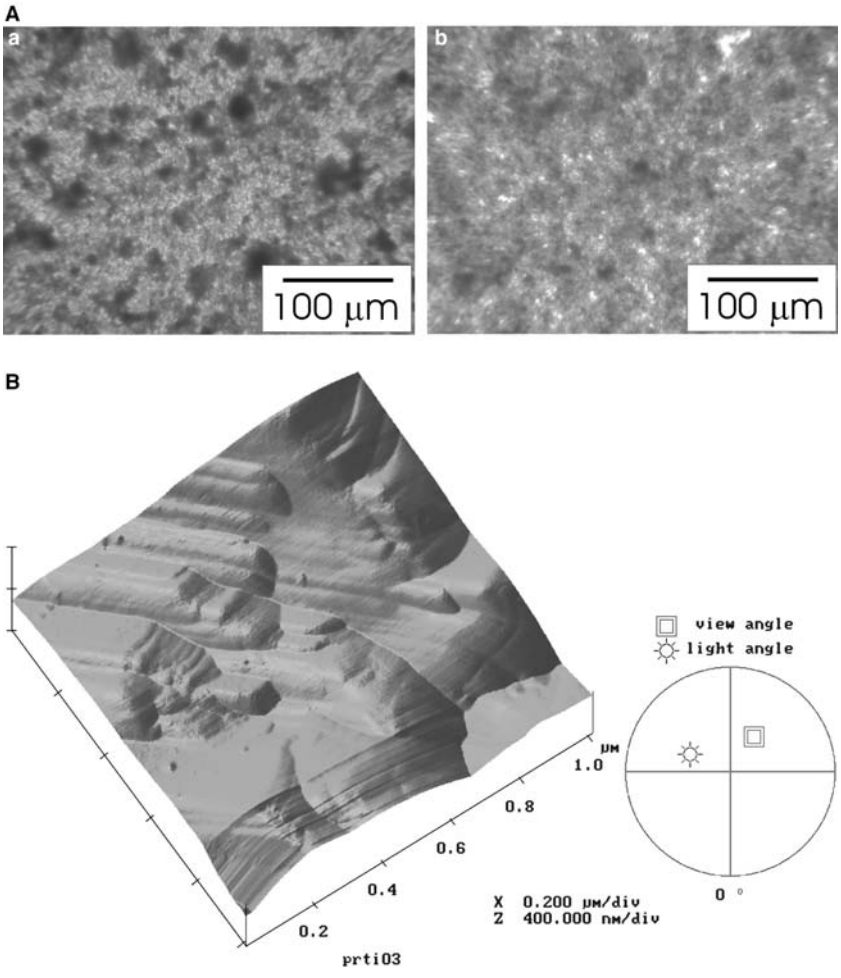

Fig. 9 **a** Optical microscopic pictures of self-assembled films at 25× magnification: **a** films built from aqueous and **b** from *n*-propanol. **b** AFM image of $H_2Ti_3O_7$ film (1μm × 1μm) prepared on a glass surface

measure the finer particles. *H*-titanate suspensions did not sediment, they were stable and easy to measure. The average particle size of hydrogen titanate was nearly identical with that of sodium titanate (570–590 nm); the size distribution of *H*-titanate, however, was significantly more monodisperse (Fig. 5).

The thermodynamical stability of the sodium titanates is excellent. Below 1,000 °C no process associated with significant mass loss or structural rearrangement other than the initial loss of the small amount of adsorbed water (2–3 wt%) takes place (Fig. 6). In the case of *H*-titanate, adsorbed water is removed sooner, below 60 °C; next, at 245 °C another endothermic process, most probably the evaporation of structural water is observed. The total mass loss up to 1,000 °C is 11.3 wt%.

The surface charge density of hydrogen titanate was determined by charge titration via adsorption of hexadecylpyridinium ions. 10 ml of 0.2 g/l titanate suspension with negative surface charge reached the value of $\xi = 0$ after the addition of 1.45 ml of 0.05 mmol/l HDPCl surfactant solution. The calculated value of surface charge density is 0.0725 mmol/g. Since X-ray diffractograms revealed a chain-dependent tendency for intercalation, this value was also determined in the presence of molecules with shorter alkyl chains. When titrated with butylamine and octylamine, the charge density was 2.2 mmol/g and 1.3 mmol/g, respectively. The value measured with butylamine most probably represents charges on the entire internal and external surface, whereas HDPCl had access only to the negative charges of the external surfaces. In the case of adsorption of HDPCl molecules no intercalation process was detected by XRD.

Investigations on self-assembled films

The film preparation by the layer-by-layer technique is illustrated in Fig. 7. The increase in the number of layers was monitored by UV-VIS absorption spectrophotometry at $\lambda = 600$ nm after the deposition of each *H*-titanate layer. As shown in Fig. 8a, the thickness of the

films increases with increase in the number of layers. The strong dependency of light absorption as a function of the deposited number of layers is evident. Line 2 shows the absorbance values if we used n-propanol (film 2) as deposition liquid. The amount of deposited titanate (mg/cm^3) of the last layer was calculated from absorbance values using a calibration curve measured at $\lambda = 600$ nm in titanate dispersions of different particle concentrations. If we assume that the particles bound preferentially on the glass surface of the cuvette, we calculate the surface concentration of particles in mg/cm^2 . The calculated surface density is 0.34 ± 0.02 mg/cm^2 for film 1 (in aqueous dispersion), and 0.17 ± 0.01 mg/cm^2 for film 2 (in propanol). These values correspond to the gravimetric measurements (0.33 mg/cm^2 for film 1 and 0.17 mg/cm^2 for film 2), using a Mettler precision balance drying the sample in N_2 gas flow. Knowing the density of *H*-titanate ($\rho = 3.1557$ g/cm^3) the calculated, layer thicknesses were 1.062 μm for film prepared in aquatic system and 0.53 μm in alcoholic system respectively.

X-ray diffractograms were recorded after the deposition of every fifth layer. After the fifth layer, the characteristic (100) reflection of *H*-titanate appeared at $d_L = 0.78$ nm; and its intensity was higher in the case of aqueous films (Fig. 8b, pattern 1). The diffractogram also displayed a higher d-value ($= 6.43$ nm) that can be associated with the distance of titanate layers in the film. On the XRD pattern 2, we see only the Bragg reflection with lower intensity (about half the intensity as in pattern 1) characteristic for *H*-titanate, because the layer thickness is also the half of the *H*-titanate/PDDA system. Light microscopic pictures (Fig. 9a, b) show the films from water to be considerably thicker and more uneven (Fig. 9a) than those prepared in n-propanol, which are thinner and more ordered (Fig. 9b). The reason is that, due to the evaporation of the alcohol, the adhesion between the titanate lamellae is stronger. The AFM picture of the self-assembly film on Fig. 10 shows very well ordered TiO_6 sheets.

Conclusions

Our experiments reveal an analogy between the intercalation and self-assembly of layer silicates and titanates. The tendency of titanates to self-assemble is described, which make titanates suitable candidates for utilization as efficient photocatalysts. It was further observed that readily evaporating dispersion solvents yield more highly ordered nanofilms than water, due to stronger adhesion between the titanate lamellae.

Acknowledgements The authors wish to thank the Hungarian National Scientific Fund (OTKA) T 034430, F 042715 and M045609, for their financial support.

References

1. Andersson S, Wadsley AD (1961) Acta Cryst 15:663
2. Andersson S, Wadsley AD (1961) Acta Cryst 14:1245
3. Easteal AJ, Udy DJ (1972) High Temperature Sci 4:487
4. Izawa H, Kikkawa S, Koizumi M (1983) Polyhedron 2(8):741
5. Sasaki T, Watanabe M, Komatsu Y, FujikiY (1985) Inorg Chem 24(14):2265
6. Beneke K, Lagaly G (1978) Z Naturforschung 33b:564
7. Lagaly G, Beneke K (1991) Colloid Polymer Sci 269:1198
8. Izawa H, Kikkawa S, Koizumi M (1982) J Phys Chem 86(25):5023
9. Feist TP, Mocarski SJ, DaviesPK, Jacobson AJ, Lewandowski JT (1988) Solid State Ionic 28-30(2):1338
10. Kikkawa S, Yasuda F, Koizumi M (1985) Mater Res Bull 20(10):1221
11. Nunes LM, Souza AG, Farias RF (2001) J Alloys Compounds 319(1-2):94
12. Airoldia C, Nunes LM, Farias RF (2000) Pergamon Mater Res Bull 35:2081
13. Ogawa M, Takizawa Y (1999) Chem Mater 11(1):30
14. Sukpirom N, Lerner MM (2001) Chem Mater 13:2179
15. Sukpirom N, Lerner MM (2003) Mater Sci Eng A 354(1-2):180
16. Yang J, Li D, Wang HZ, Wang X, Yang XJ, Lu LD (2001) Mater Lett 50(4):230
17. Cheng S, Tsai SJ, Lee YF (1995) Catalysis Today 26(1):87
18. Zheng S, Yin D, Miao W, Anderson GK (1998) J Photochem Photobiol A Chem 117(2):105
19. Morawski AW, Grzechulska J, Kalucki K (1996) Phys Chem Solids 57(6-8):1011
20. Sato T, Yamamoto Y, Fujishiro Y, Uchida S (1996) J Chem Soc Faraday Trans 92:5089
21. Sato T, Masaki K, Sato K, Fujishiro Y, Okuwaki A (1996) J Chem Tech Biotechnol 67:339
22. Fujishiro Y, Uchida S, Sato T (1999) J Inorg Mater 1:67
23. Yanagisawa M, Sato T (2001) Int J Inorg Mater 3(2):157
24. Yanagisawa M, Uchida S, Sato T (2000) Int J Inorg Mater 2(4):339
25. Shangguan W, Yoshida A (2001) Solar Energy Mater Solar Cells 69(2):189
26. Machida M, Ma XW, Taniguchi H, Yabunaka J, Kijima T (2000) J Molec Catalysis A Chem 155(1-2):131
27. Harada M, Sasaki T, Ebina Y, Watanabe M (2002) J Photochem Photobiol A Chem 148:273
28. Sasaki T, Ebina Y, Tanaka T, Harada M, Watanabe M, Decher G (2001) Chem Mater 13(12):4661
29. Ramírez-Salgado J, Fabry P (2003) Solid State Ionics 158:297
30. Ramírez-Salgado J, Djurado E, Fabry P (2004) J Eur Ceramic Society 24:2477
31. Holzinger M, Maiera J, Sitteb W (1996) Solid State Ionics 86-88:1055
32. Dékány I, Szántó F, Weiss A, Lagaly G (1986) Ber Bunsenges Phys Chem 90:422
33. Lagaly G, Weiss A (1971) Kolloid-Z. U. Z. Polymere 243:48
34. Lagaly G, Weiss A (1971) Kolloid-Z U Z Polymere 248:968